

REPORT DOCUMENTATION PAGE

Form Approved

OMB No. 0704-0188

Public reporting burden for this collection of information is estimated to average 1 hour per response, including the time for reviewing instructions, searching existing data sources, gathering and maintaining the data needed, and completing and reviewing the collection of information. Send comments regarding this burden estimate or any other aspect of this collection of information, including suggestions for reducing this burden, to Washington Headquarters Services, Directorate for Information Operations and Reports, 1215 Jefferson Davis Highway, Suite 1204, Arlington, VA 22202-4302, and to the Office of Management and Budget, Paperwork Reduction Project (0704-0188), Washington, DC 20503

1. AGENCY USE ONLY (Leave blank)

2. REPORT DATE
Sept, 1, 19963. REPORT TYPE AND DATES COVERED
Final Report, June 1, 1994-May 31, 1996

4. TITLE AND SUBTITLE

A Microactuator/Microsensor System For The Study And Control of Screech in High Speed Jets

5. FUNDING NUMBERS

F49620-94-0184

94-1-0184

6. AUTHOR(S)

Khalil Najafi

7. PERFORMING ORGANIZATION NAME(S) AND ADDRESS(ES)

The Regents of The University of Michigan
Ann Arbor, MI 48109

AFOSR-TR-96

0530

9. SPONSORING/MONITORING AGENCY NAME(S) AND ADDRESS(ES)

Air Force Office of Scientific Research (AFOSR)
Bolling AB, Washington DC 20332-6448

NA

10. SPONSORING/MONITORING AGENCY REPORT NUMBER

11. SUPPLEMENTARY NOTES

The views and conclusions contained herein are those of the authors and should not be interpreted as necessarily representing the official policies or endorsements, either expressed or implied, of the Air Force Office of Scientific Research or the US Gov

12a. DISTRIBUTION/AVAILABILITY STATEMENT

Distribution Statement A. Approved for public release; distribution is unlimited.

12b. DISTRIBUTION CODE

13. ABSTRACT (Maximum 200 words)

A novel Micro-Electro-Mechanical Actuator was designed, fabricated, and tested for the control of screech in high-speed jets. It was used at the exit of a supersonic axisymmetric jet for the introduction of perturbations into the convectively unstable supersonic shear layer. The 14-micron thick electrostatic microactuator was fabricated using bulk micromachining from a boron-doped silicon wafer which was bonded to a support glass substrate. The actuator could be forced into mechanical resonance at a frequency of 5kHz at an amplitude of more than 70 microns peak-to-peak using a 20V DC and a 20V AC voltage drive. The actuator and its sense and drive electronics were mounted on a printed circuit board, and several of these boards were mounted at the exit lip of a high-speed jet flow system. The entire system was tested at different jet speeds of up to 100 m/s, and disturbances were introduced into the jet flow as measured using hot wire anemometers placed downstream from the jet nozzle. Two different actuator designs were fabricated, with the second providing better resistance to breakage at high speeds. Ongoing investigations are aimed at developing a technique to modify, and ultimately control, the feedback loop responsible for the creation of screech.

14. SUBJECT TERMS

Screech, Microactuator, Microelectromechanical Systems

15. NUMBER OF PAGES
19

16. PRICE CODE

17. SECURITY CLASSIFICATION OF REPORT

UNCLASSIFIED

18. SECURITY CLASSIFICATION

UNCLASSIFIED

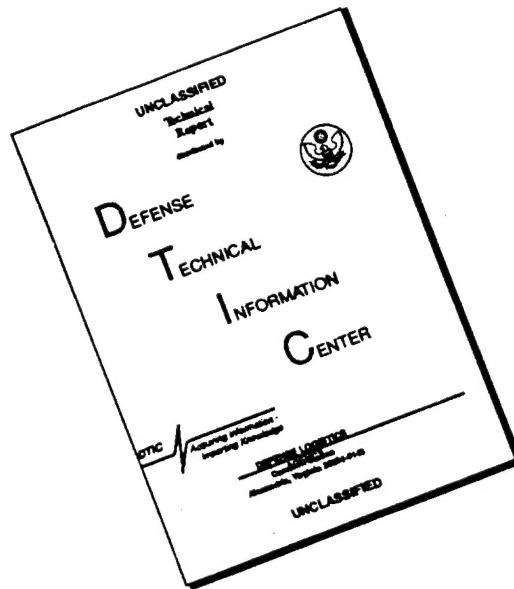
19. SECURITY CLASSIFICATION OF ABSTRACT

UNCLASSIFIED

20. LIMITATION OF ABSTRACT

UL

DISCLAIMER NOTICE



THIS DOCUMENT IS BEST QUALITY AVAILABLE. THE COPY FURNISHED TO DTIC CONTAINED A SIGNIFICANT NUMBER OF PAGES WHICH DO NOT REPRODUCE LEGIBLY.

***A Microactuator/Microsensor System For The
Study And Control Of Screech In High Speed Jets***

Final Technical Report

Submitted to

Air Force Office of Scientific Research
Bolling AFB, Washington DC 20332-6448

Grant Number: F49620-94-0184
Period Covered: 6/1/94-5/31/96

Submitted By:

Center for Integrated Sensors and Circuits
Department of Electrical Engineering and Computer Science
University of Michigan
Ann Arbor, Michigan 48109-2122

Technical Contact:
Professor Khalil Najafi, Principal Investigator
1246B EECS Building, 1301 Beal Avenue
Ann Arbor, MI 48109-2122
Tel: (313) 763-6650; FAX: (313) 647-1781
e-mail: najafi@engin.umich.edu

Administrative Contact:
Dr. Neil D. Gerl
Division of Research Development and Administration
Room 1058, Wolverine Tower
3003 S. State Street
Ann Arbor, MI 48109-174
Tel: (313) 763-6438

August 1996

19961104 093

I. Introduction

Development of advanced aircraft requires not only a detailed understanding of the physics of turbulence and fluid dynamics, but also a means to prevent unsteady and potentially dangerous flow conditions. An area of interest in turbulence research is that of receptivity theory of the coupling of acoustic waves and shear flow and the screech phenomenon of supersonic jets operated at off-design condition [1-3]. Screech is a resonant feedback condition that occurs when shear-layer instability waves interact with the shock system of a supersonic plume. The feedback loop consists of shear-layer disturbances convecting through the system of shock cells. Interaction of the disturbances with the shock cells produces acoustic waves that propagate upstream outside the shear-layer to the nozzle lip. At the nozzle lip shear-layer disturbances are generated by the acoustic waves through receptivity thus completing the loop (as shown in Figure 1). Figure 2 shows the power spectra, obtained from microphone data taken from a supersonic jet, that illustrates the screech phenomenon. The feedback loop causes lock-in to a resonant frequency and so screech appears as a high intensity peak in the spectrum at a sharply defined frequency. The energy balance in this process controls the acoustic amplitude and is dependent on parameters such as instability wave growth rate, shock strength, instability-wave mode shape, wave convection velocity, external flow velocity, aft-body acoustic reflection characteristics, fuselage boundary layer characteristics, jet velocity distribution, and the receptivity of the shear layer to acoustic perturbations, among others. This project aimed at developing a microactuator using the emerging technology of Micro-Electro-Mechanical Systems (MEMS) to explore a novel method of flow control, particularly in introducing disturbances into a compressible shear layer and hence controlling the formation of screech.

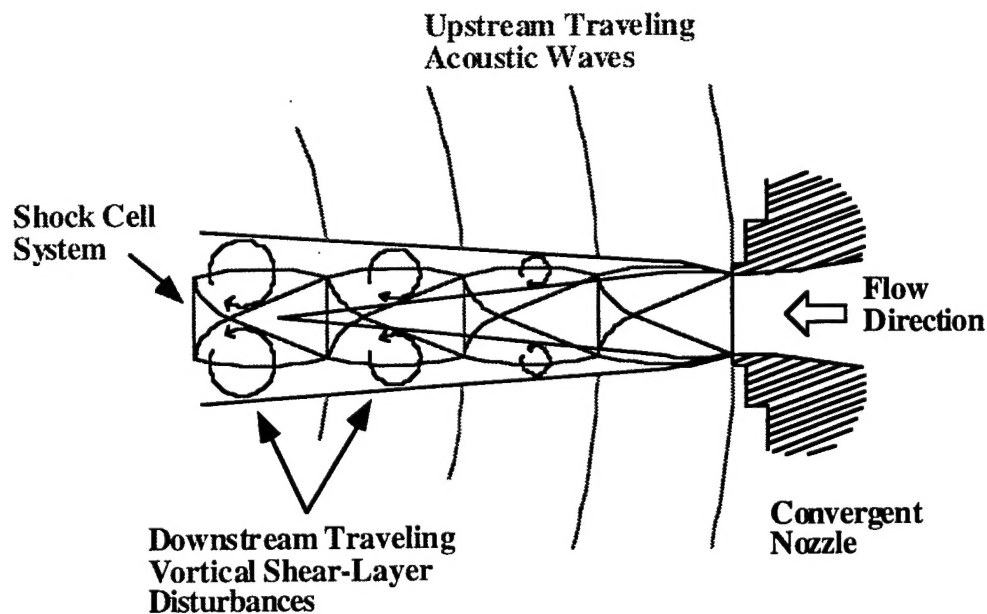


Figure 1: Illustration of screech in high-speed jets.

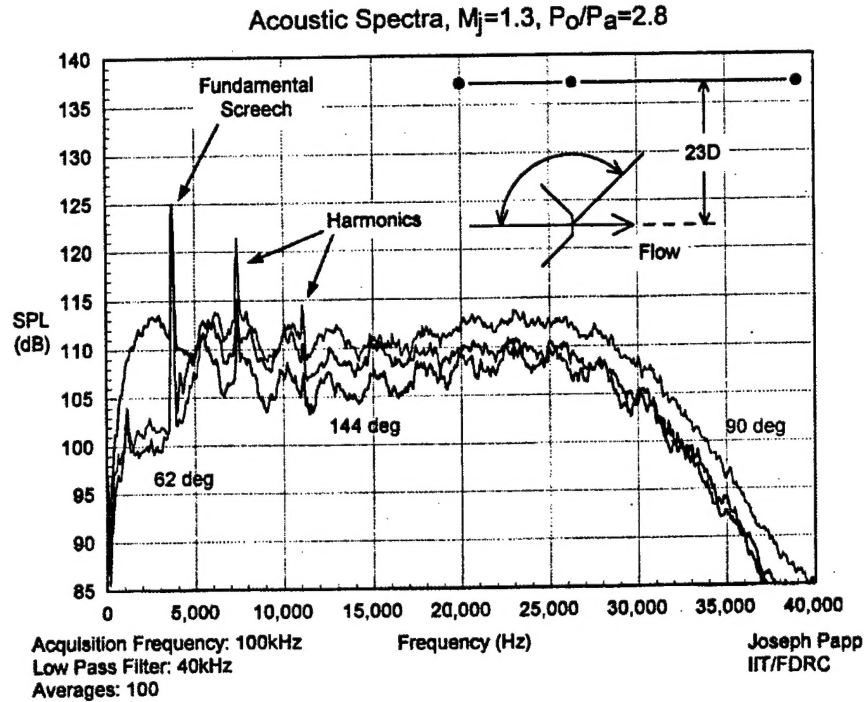


Figure 2: The power spectra obtained from microphone data taken from a supersonic jet.

The coupling of acoustic waves and free shear flows requires that local wavelength match be achieved between the incident acoustic field and the instability waves that develop in the shear layer. Recently, receptivity theory has been developed which suggests mechanisms for this coupling phenomenon. It is widely known that incompressible shear layers can be excited by an incident acoustic field. However, similar coupling has been more difficult to achieve in compressible shear flows, even when the reduced growth rate of shear layer disturbances is considered. It is conjectured that acoustic refraction through a high-speed shear layer is at least partially responsible for the diminished receptivity. By using an array of microactuators it is possible to interfere with the screech feedback loop at the point of receptivity where the compressible shear layer disturbances are created by acoustic waves at the nozzle lip. The microactuator array is designed to effectively replace the original nozzle lip with one that can produce different types of disturbance modes, as shown in Figure 3. Figure 4 shows the overall configuration of the microactuators in the high speed jet and a magnified view of one of the MEMS devices. The actuators are mounted on the jet lip with their motion aligned radially to the jet axis in the exit plane. Theoretically, the actuator array could induce perturbations to modify the Kutta condition at the lip of the nozzle to explore the controllability of the shear layer instability through such manipulations. Then instability waves will be driven out of phase with the fundamental screech instability mode to cancel the screech tone completely.

The frequency of the fundamental screech tone for the one inch nozzle in the High Speed Jet Facility at the Fluid Dynamics Research Center, Illinois Institute of Technology, decreases from approximately 9.5 kHz near Mach 1.0 to 4.5 kHz at Mach 1.6. The jet Mach number at which screech experiments would be conducted would therefore determine the resonant frequency of the actuator. In addition the smooth decrease in screech frequency is interrupted by regions

where no discrete frequency exists and by discontinuous jumps in frequency where a new instability mode becomes the one most amplified.

We have chosen an actuator frequency of 5.0 kHz, which corresponds to a region of smooth change in screech frequency. In addition, this value was chosen to take advantage of one of the discontinuous frequency jumps. Because of the discontinuity, 5.0 kHz actually corresponds to two distinct jet Mach numbers at approximately 1.31 and 1.49. This widens the scope of experimental applications of the actuators by allowing the study of two different jet instability modes.

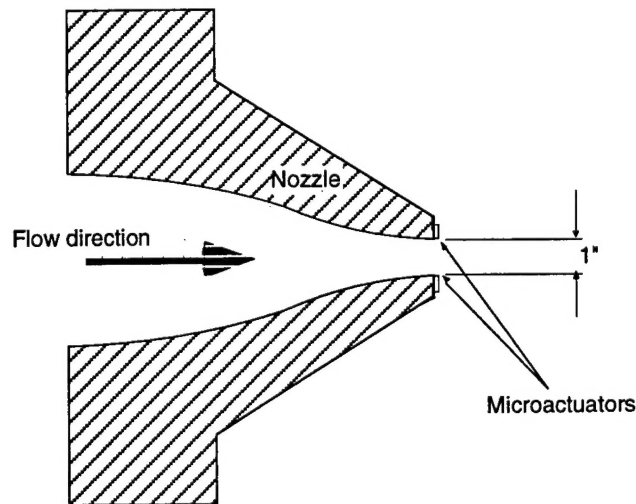


Figure 3: Closed-loop control of screech in a high-speed jet using microactuators placed on the jet nozzle.

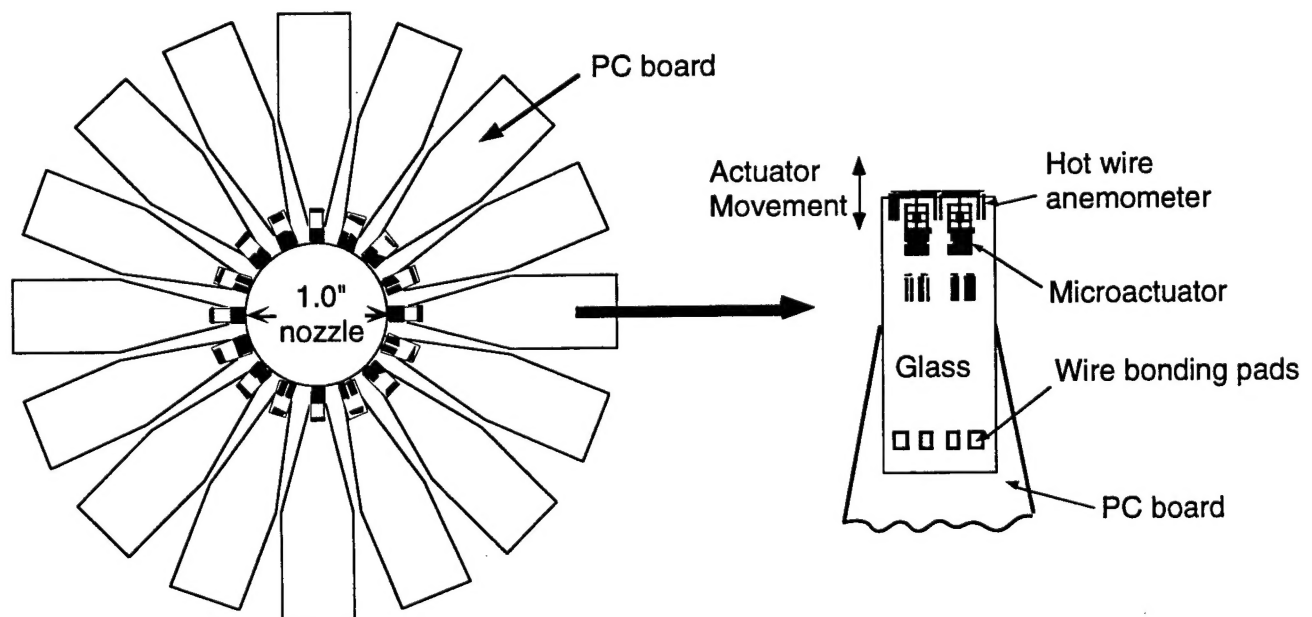


Figure 4: The overall structure of the microactuator/microsensor system. The system consists of a number of microactuators and hot wire anemometers that are all fabricated on a glass substrate and are located around a 1.0" diameter hole.

This basic research effort is conducted in with colleagues at the Fluid Dynamics Research Center of the Illinois Institute of Technology (FDRC/IIT). The ultimate goal of this work is to develop a MEMS-based system and utilize it on the High Speed Jet Facility (HSJF) at IIT and conduct research into the active modification and control of screech in supersonic shear layers. This report presents a summary of the results that have been obtained during the past two years.

II. Experimental Approach

As mentioned before, it is understood that the screech phenomenon is caused by a feedback loop consisting of three components: 1) downstream propagating shear layer instabilities; 2) shock cell structure in the supersonic jet plume; and 3) upstream-propagating acoustic waves outside of the jet. Experimental investigations indicate that the shear-layer is driven by interaction with the acoustic waves and amplifies the resulting small disturbances, causing the lock-in effect that leads to the resonant condition responsible for screech. This indicates two points that motivate our experimental approach: 1) the supersonic shear layer is receptive to the acoustic frequencies and small amplitudes of acoustic waves, and 2) it is unstable to, and therefore capable of amplifying, such acoustic perturbations.

The first goal of the experimental approach was to determine the conditions under which the MEMS actuator-generated perturbations can be made to interact with the supersonic shear layers near the lip of the jet. The perturbations introduced by the actuators will then be amplified by the natural convective instability of the shear layers, and allow for the possibility that the introduction of controlled perturbations using the MEMS actuators which can be used to control the convective instability of the shear layer. The effectiveness of the actuators at modifying the Kutta condition seen by the flow at the nozzle trailing edge, and the receptivity of the flow to such modification need to be determined.

In order to explore the effectiveness of using the MEMS actuators at the nozzle trailing edge, an actuator array consisting of four devices (eight actuators) could be evenly spaced around the circumference of the jet exit. This could be used to investigate the interaction of the actuator generated perturbations with the supersonic shear layer, particularly the receptivity of the flow at the nozzle trailing edge to such disturbances. The flow is documented using well-known measurement techniques used for compressible flow. These include the measurement of flow velocities using constant temperature hot wires, acoustic measurements using precision microphone equipment, and short duration shadowgraph flow visualization of the jet structure, the acoustic wave structure and the MEMS induced perturbations.

Investigations of the four-MEMS array could then be followed by investigations using a larger array of 16 MEMS devices (32 actuators) evenly spaced around the jet exit (as shown in Figure 4). The understanding obtained from the investigations using the four-device array of the receptivity of the supersonic shear layer to the MEMS-induced modifications of the Kutta condition at the nozzle trailing edge could be extended through investigations of the response of the shear layer to simultaneous perturbation at each point of the nozzle lip. These 32 independently controllable actuators allow for phase differences between the various actuators, thus permitting investigation not only of two dimensional axisymmetric disturbances (when the phase difference is zero), but virtually any three dimensional perturbation (when the phase varies around the lip).

One of the goals of this research was to investigate the possibility of using MEMS actuators for modifying the convective instability of the shear layer and affecting the screech feedback loop. Control strategies using the MEMS actuators as the active elements in a control loop, and the on-chip sensors or external sensors for feedback, could be investigated for the control and

modification of the feedback loop of the jet itself. This offers the possibility for active control of the screech phenomenon.

III. High Speed Jet Facility

The High Speed Jet Facility at the Illinois Institute of Technology Fluid Dynamics Research Center consists of a one inch diameter axisymmetric nozzle exhausting into an anechoic chamber (as shown in Figure 5). The anechoic chamber is actually an anechoic duct, as it is open the ends normal to the jet axis to accommodate the high flow and entrainment rates that are present in supersonic jet flow. The 7,000 ft³ compressed air supply system provides a maximum exit pressure ratio of 14.6 and fully expanded Mach number of 2.4. Jet exit conditions are maintained as supply tank is depleted by a segmented ball control valve and a proportional-integral-differential (PID) digital control loop. Flow conditioning and two fifth order polynomial contractions within the jet body ensure a high quality laminar exit flow. The anechoic chamber is designed with optical access windows for high-speed shadowgraph and Schlieren flow visualization. The jet exit is designed to facilitate the mounting of an array of 16 actuator chips for a total of 32 actuators around inner nozzle diameter.

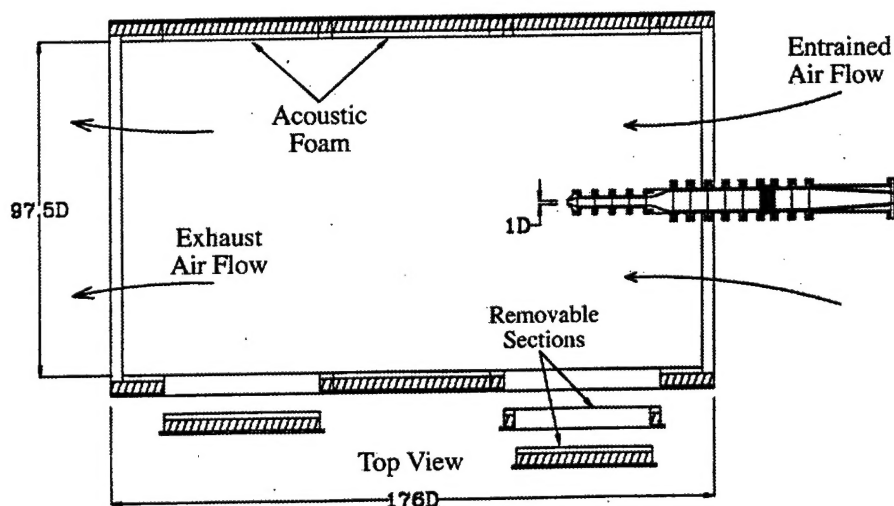


Figure 5: The high-speed jet facility at IIT.

IV. Microactuator Structure

In order to generate sufficient mechanical perturbations into the jet plume at the correct resonant frequency, the actuators should be 1-2mm wide, should not introduce unwanted perturbations (such as thermal) into the jet, should be able to interact with the shear layer of the jet flow by physically intruding into the shear layer, and should be capable of tens of microns of movement at its resonant frequency. This requires that the front portion of the actuator tip overhangs the edge of its substrate and enters the shear layer of the jet flow when activated (as shown in Figure 4). Because the screech phenomenon occurs at a velocity for Mach numbers of 1.31 and 1.49, a MEMS device needs to be developed that is capable of functioning in the relatively harsh environment present at the lip of the supersonic jet. Indeed, this is a very challenging task since the jet speeds could approach several hundred meters per second, the flow

can contain many particulates that can easily damage the microactuator, and above all, the microactuators are extremely small and delicate devices that have never before been operated under these conditions. These conditions dictate that the actuator must be very compliant in the direction parallel to the substrate, and very stiff perpendicular to the substrate. In order to achieve these requirements, electrostatic actuators that are supported by thick, narrow and long beams can be utilized. Electrostatic actuation is desirable because one can achieve relatively large motions in a small area without generating unwanted thermal disturbances. The large thickness required for large stiffness in one direction can be achieved by using thick micromachined bulk silicon microstructures. In addition, because of their small mass and rather stiff supports, these actuators can be resonated at the relatively high frequencies of 5kHz.

Figure 6 shows the overall view of a single actuator. The actuator is fabricated from boron-doped silicon which is supported on a glass substrate [4]. The microstructure is formed using a high aspect-ratio reactive ion etching process on a silicon wafer that is doped with high concentrations of boron. The silicon wafer is electrostatically bonded to a glass substrate which supports interconnect metal lines, and is dissolved away to leave the microstructure supported on the glass substrate. This will allow for the overhang of the actuator tip. In addition, a large air gap can be formed between the silicon and the glass substrate in order to reduce clamping. The microactuator tip is supported by narrow folded beams that are attached to the substrate at the anchor points. The overall device can be driven into resonance by applying an AC voltage between comb fingers that are formed in both the moving microactuator mass and drive electrode that are attached to the glass substrate. As shown, it is also possible to form miniature hot wire anemometers using the same boron-doped silicon so that flow conditions around the microactuator can be measured.

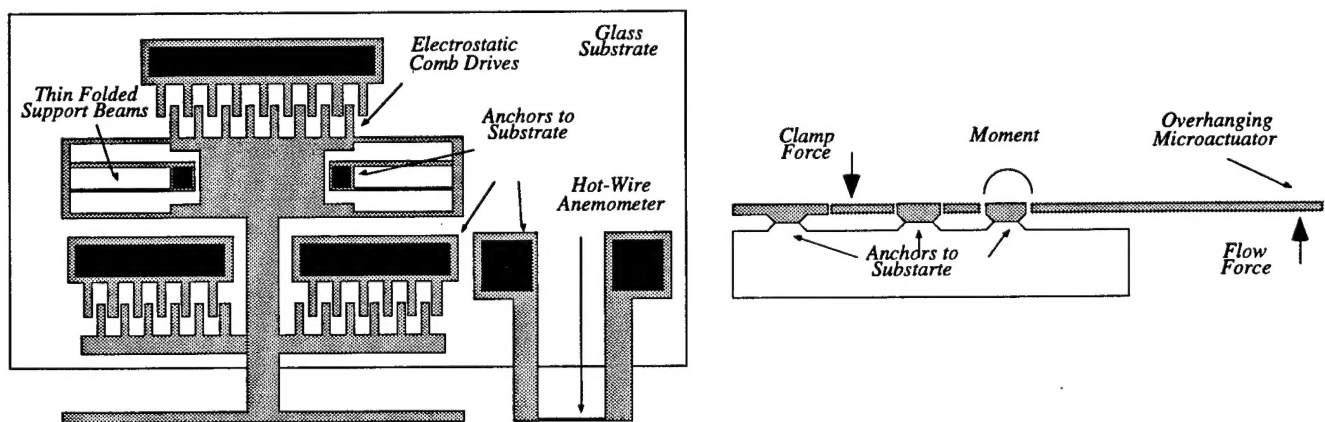


Figure 6: The top and side views of the structure of the electrostatic microactuator.

V. Fabrication

Figure 7 shows the complete dissolved-wafer process which is used to fabricate these actuators. The actuator itself is fabricated from micromachined p++ silicon microstructures that are supported on a glass substrate. The head of the actuator is located in the proper position

overhanging the edge of the glass substrate and interacts with the jet flow, as required in this application. The fabrication process of the device requires four masks. It starts by recessing the silicon wafer with KOH (an orientation-dependent silicon etchant) [4] to a depth of a few microns, except in areas that will later be bonded to the glass substrate to anchor the actuators. Next an unmasked deep boron diffusion ($\sim 12\mu\text{m}$) is performed at 1175°C for 15 hours, which defines the thickness of the beams and the teeth of the drive combs. The large thickness is critical to this application since it reduces both the drive voltage and the susceptibility to clamping. The wafer is then patterned and metalized with a Ti/Pt layer in areas where lead transfers are to be created to the metal lines on the glass substrate. The boron-diffused areas are then etched anisotropically using reactive ion etching (RIE) in a SF_6 gas plasma to pattern the fine microstructures needed to form the support beams and the drive combs [4]; this completes silicon processing. The glass substrate is patterned and recessed to a depth of about $6\mu\text{m}$ by a mixture of diluted hydrofluoric (HF) and nitric acids to create the bonding anchors. This recess is also critical as it allows the formation of a gap under the silicon structure which is large enough to reduce the clamping of the microactuator to the substrate both during processing and later in operation. The formation of such a gap is practically possible only by using the dissolved wafer process. Glass processing is completed after patterning Ti/Pt/Au interconnect lines on it. Finally, the silicon wafer is electrostatically bonded to the glass wafer, and the sandwich is then immersed in EDP (a concentration-dependent silicon etchant) to dissolve away the undoped silicon, leaving the p++ silicon devices mounted on the glass substrate.

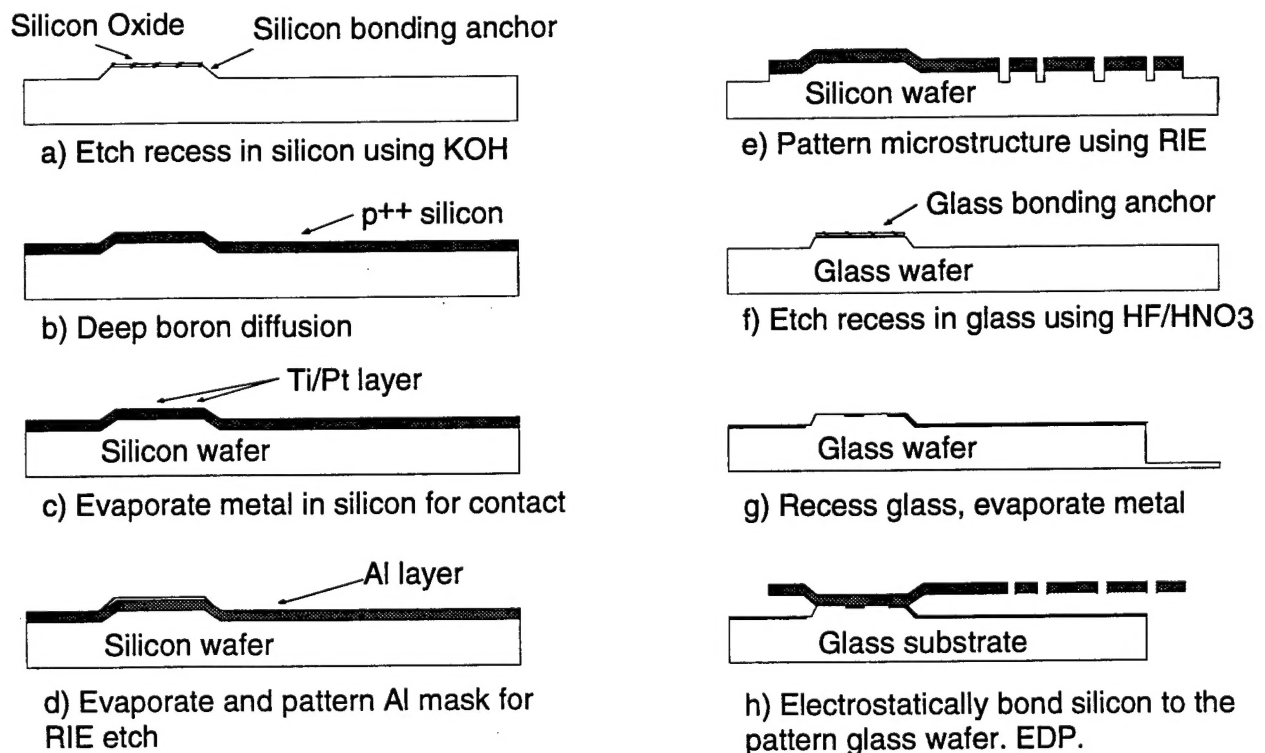


Figure 7: The dissolved-wafer process sequence for the fabrication of microactuator.

Figure 8 shows an SEM view of one of the first-generation microactuators with a hot wire anemometer on the left hand side. These actuators have been now fully tested and we have been able to obtain resonant frequencies in the range from 5kHz to over 15kHz. The resonant frequency can be changed by either changing the width of the support beam for the microactuator, or by changing the DC bias voltages between two comb fingers to electronically shift the resonant frequency. As will be discussed later, a second-generation microactuator was also fabricated which can withstand higher jet speeds.

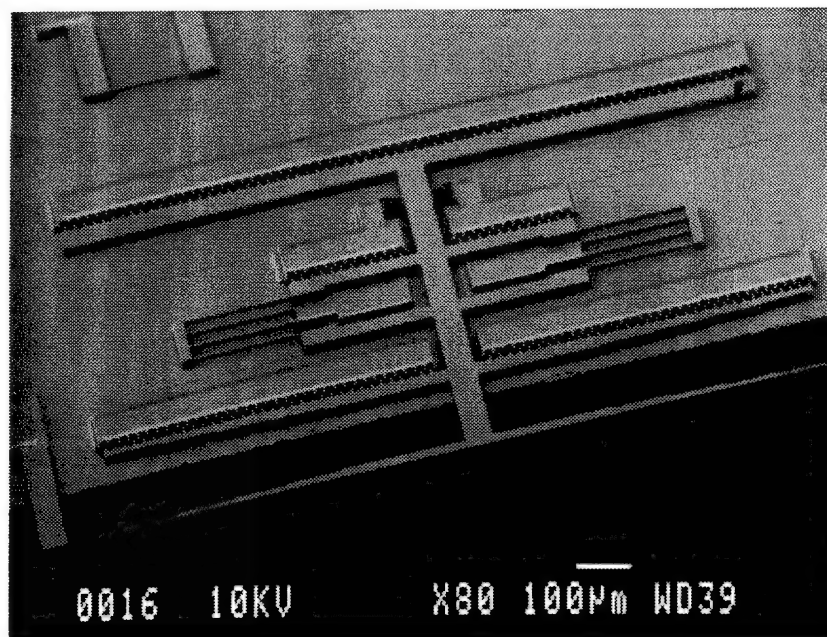


Figure 8: SEM view of the electrostatic silicon microactuator. The actuator is supported on a glass substrate and can be resonated parallel to the substrate by applying a ac voltage between the resonant mass and the comb drive electrodes. Note that the resonant part is separated from the glass by a distance of about 5 μ m.

VI. Experimental Results

After the microactuators are fabricated, they are mounted on printed circuit boards, and electrical connections to the various elements of the microactuators are created using wire bonding to the PC board. The PC boards are then ready to be mounted on the high-speed jet. Figure 9(a) shows four MEMS chips mounted on printed-circuit boards and attached to the nozzle. Figure 9(b) shows the experimental setup for incorporation of the microactuator into the jet facility. It consists of a number of microactuators and hot-wire anemometers that are fabricated on the glass substrate. The printed circuit board is mounted with the microactuator motion aligned radially to the jet's axis in its exit plane on the convergent nozzle of a high-speed jet. In order to monitor the operation of the microactuator during testing, a custom-designed circuit which is used to detect the small amplitude of the resonant actuator is attached directly on the back side of each actuator PC

board (shown in Figure 10). Figure 11 shows drive and detection electronics and the output voltage from one of these actuators as a function of frequency, showing the resonant peak. As can be seen, a function generator produces the AC signal that is passed through the simple transistor amplifier to generate the necessary high voltage and then fed into one terminal of the actuator. The current from the other terminal of the actuator is fed into a transresistance amplifier which converts the AC current through the actuator into an AC voltage that is picked up externally. These devices have been tested on the high-speed jet facility mentioned above. Table 1 summarizes the measured results for this microactuator. In addition to driving the actuator into resonance, it is also required that the operation of the actuator be monitored *in-situ* while the jet is on. This is a very important and non-trivial task because at higher jet speeds it is possible that the actuator may stop working and it is absolutely necessary that its operation be verified. Therefore, two approaches were developed to determine whether the actuator is operating *in-situ* at high jet speeds ($\approx 400\text{m/sec}$). In the first approach, we resonate the actuator electrostatically by applying an AC voltage between the two opposite comb fingers, and then monitor the AC current flow between the combs. Note that since the actuators are driven to very large amplitudes, they behave nonlinearly and generate higher frequency harmonics. Therefore, by observing the higher frequency harmonics, it is possible to determine whether the actuator has stopped or not. Figure 12 shows the frequency spectra of the actuator output when it is freely running (solid line), and when it is stopped using a probe tip (dashed line). Note that the actuator is resonating at a frequency of $\sim 5\text{kHz}$ and a peak is present both when the actuator is running and stopped (the solid and dashed lines are superimposed). However, at the first harmonic of 10kHz , we can clearly see that there is a large peak when the actuator is running, but there is no signal when it is stopped. In addition to this approach, our colleagues at IIT have also been developing an optical setup to visually observe actuator operation *in-situ*. In this system, a mirror is placed in front of the jet (at some distance), and the actuator is lit by a strobe light operating at actuator's resonant frequency. The reflected light from the actuator is passed through a lens and focused on a screen. Thus, it is possible to actually observe and see if the actuator is running.

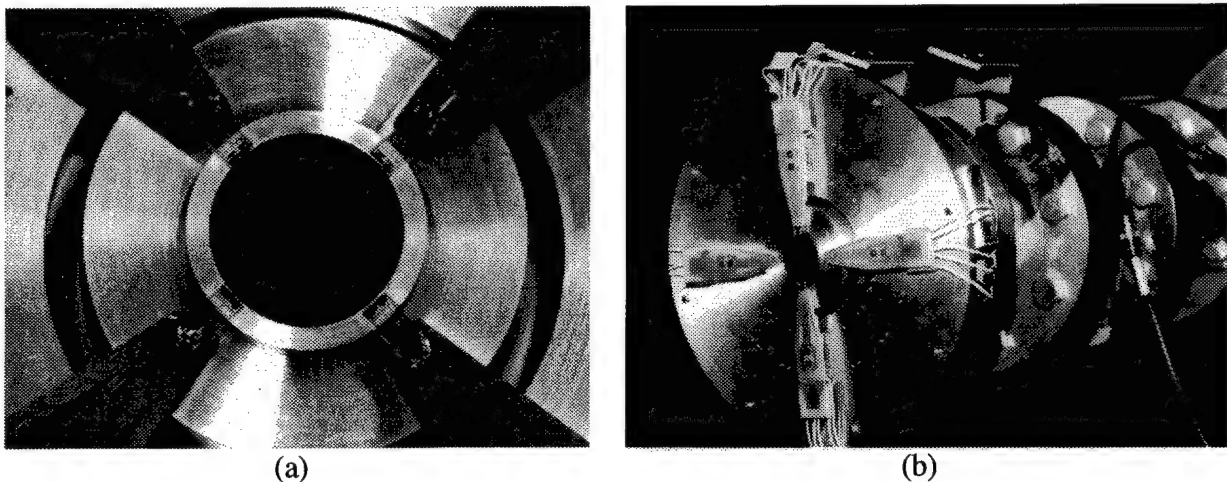


Figure 9: (a) Actuator chips mounted on a PC board, which is attached to the front surface of the nozzle. This device has been tested on a high-speed jet facility. (b) Experimental setup for incorporation of the microactuator into the jet facility, showing the jet nozzle.

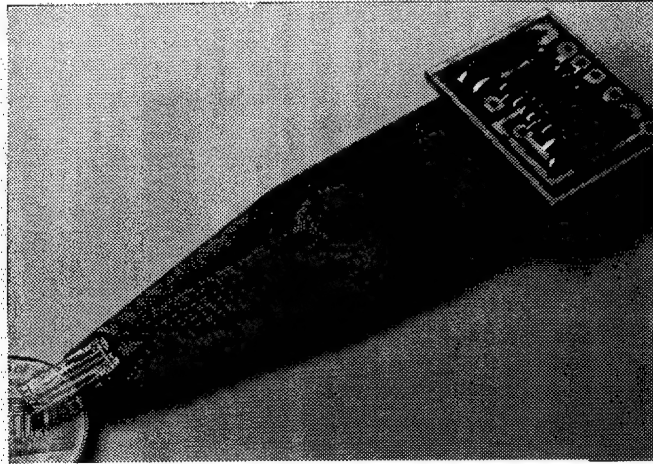


Figure 10: The microactuator chip mounted on a PC board, and the hybrid readout circuitry. To demonstrate it better, the readout circuitry is attached on the front side of the printed-circuit board.

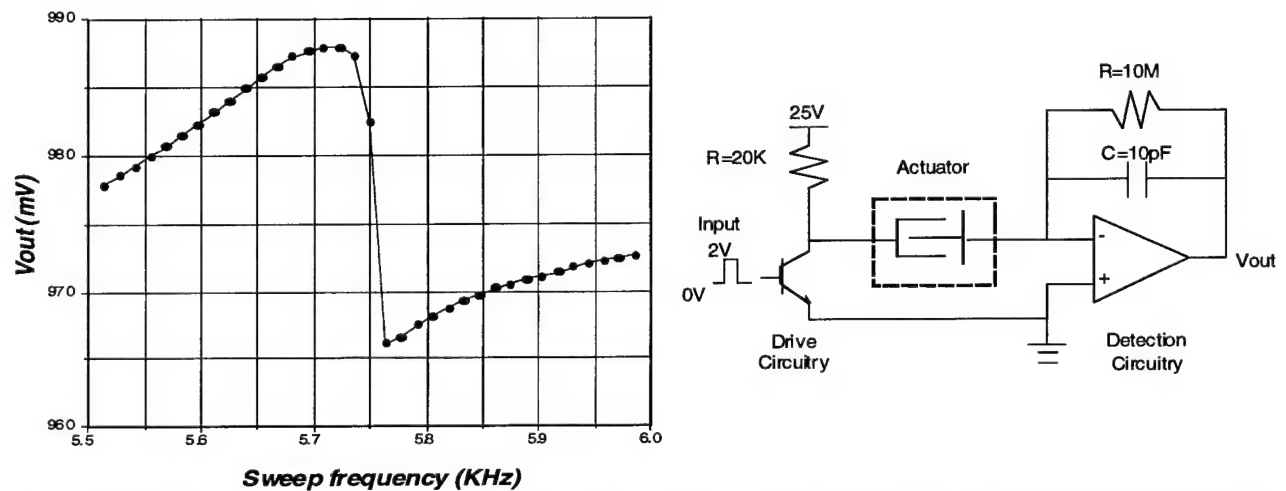


Figure 11: Measured resonant peak of one of the actuators, along with the drive and detection circuitry developed for *in-situ* monitoring of the actuator during actual use.

Table 1: Measured results from the first-generation microactuator.

		200 μm -long-folded beams*
Resonant frequency		5.45 kHz
Amplitude	$V_D=10\text{V}$ pulse	2 μm P-P
Amplitude	$V_D=20\text{V}$ pulse	9 μm P-P
Amplitude	$V_D=30\text{V}$ pulse	17 μm P-P

Beam Thickness: 11 μm , Beam Width: 4.5 μm

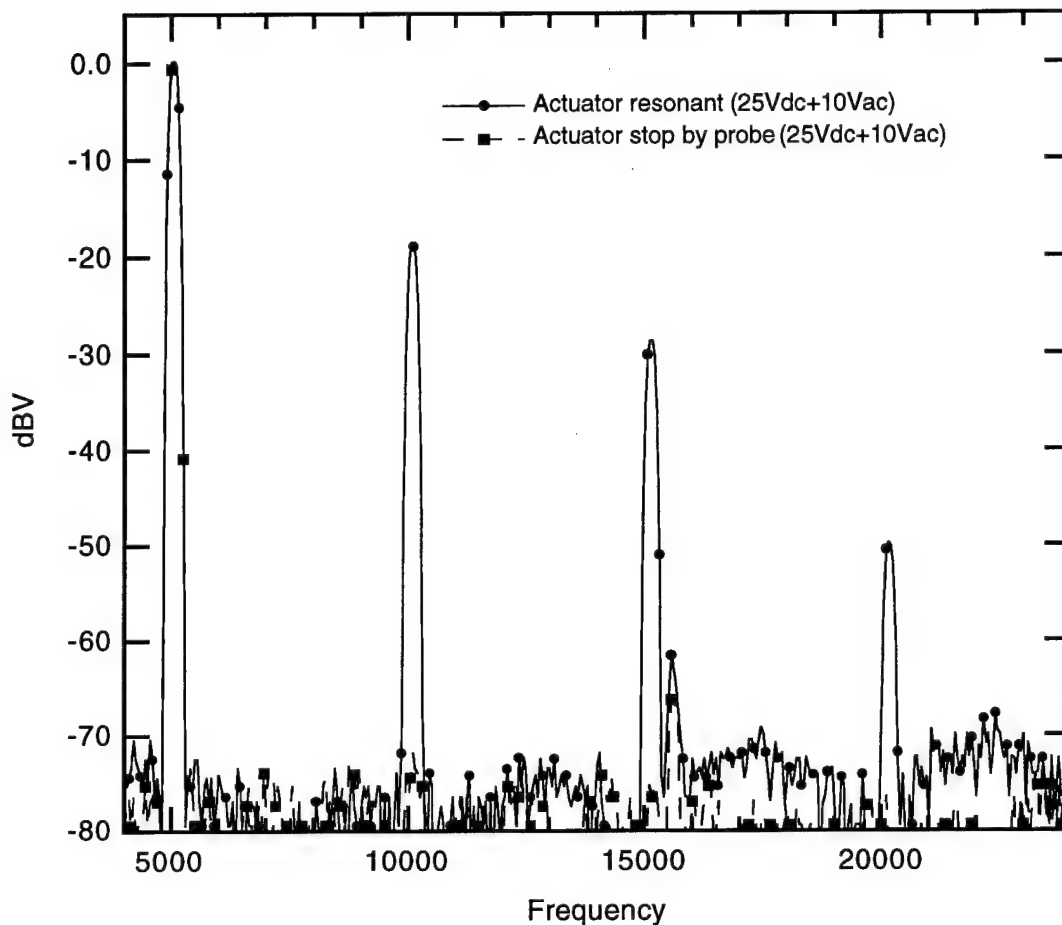


Figure 12: Spectrum results for running and stopped actuator.

Figure 13 shows the shear layer velocity fluctuations generated by this first-generation electrostatic actuator and measured by a hot-wire anemometer positioned 9mm downstream to the nozzle lip. As can be seen, the actuator generates a disturbance which travels downstream inside the shear layer at its resonant frequency ($\sim 5\text{kHz}$). Although this initial test was encouraging in that it is demonstrated that disturbances of a desired frequency can be generated and coupled into the shear layer, we also observed that at jet velocities higher than about 25m/s the actuator stopped working when it was brought to within a distance of $200\mu\text{m}$ of the edge of the nozzle lip. At supersonic velocities of $\sim 400\text{m/s}$, the actuator stopped operating within a distance of $1\text{-}1.5\text{mm}$ of the edge of the nozzle lip. This we believe was caused by the large moment forces acting on the actuator head as it is brought closer to the high-speed jet, as illustrated in Figure 6. These large forces tend to rotate the actuator out of plane and cause the rear end of the actuator to touch the glass substrate that supports the mass.

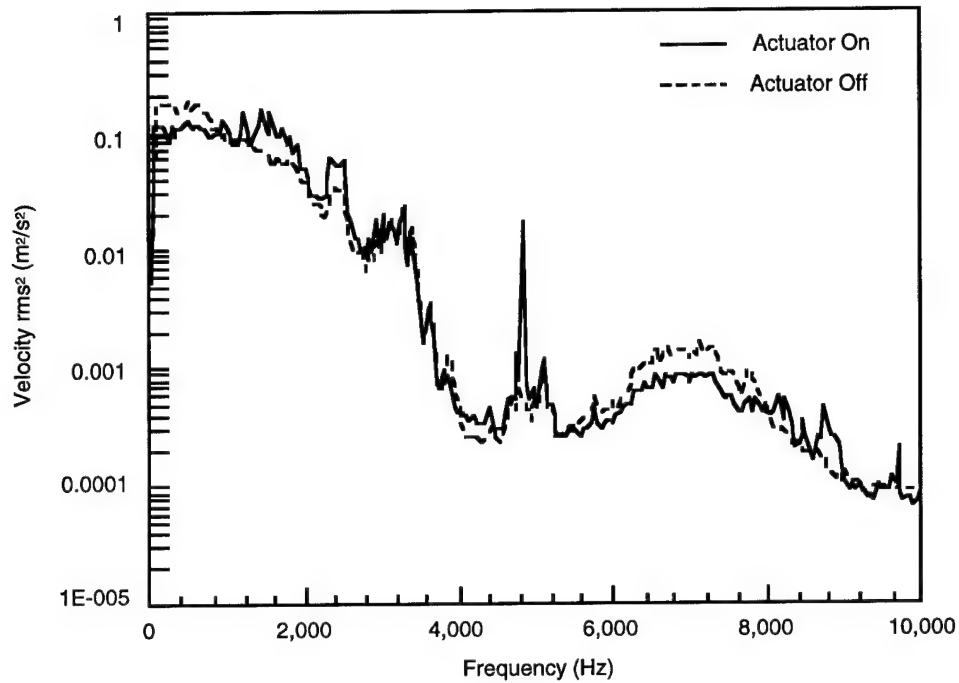


Figure 13: Shear layer velocity fluctuations measured by a hot-wire positioned 9mm downstream to the nozzle lip. As can be seen, the actuator generates a disturbance at its resonant frequency (~5kHz), which travels downstream inside the shear layer.

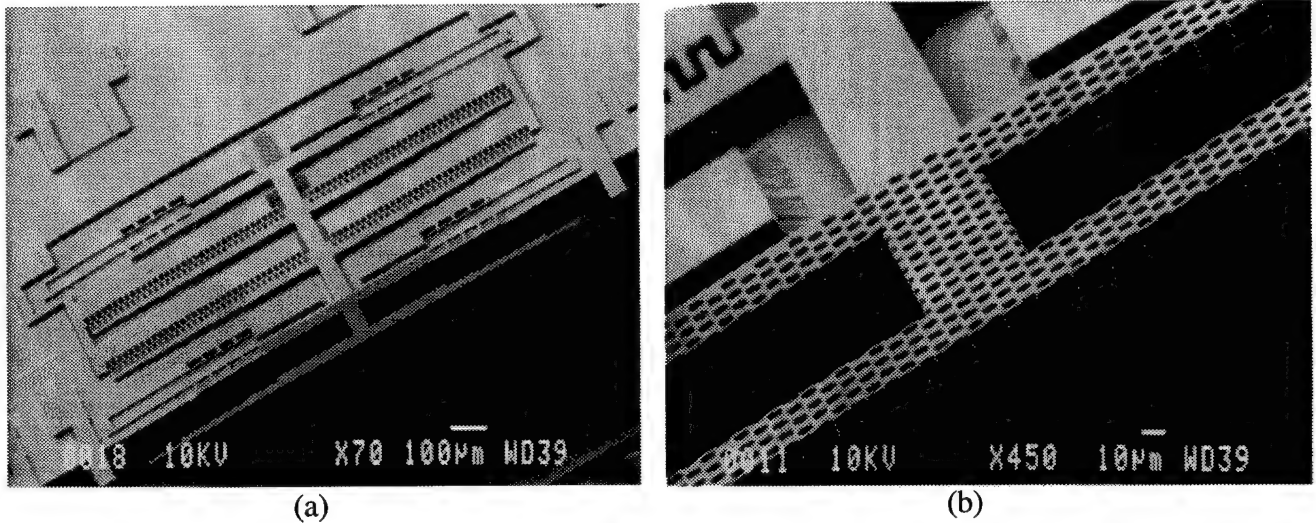


Figure 14: SEM views of the electrostatic actuator designed for controlling screech. The device is 1.3mm wide, 10µm thick. Note that the resonant part is separated from the glass by a distance of about 6µm. A close-up view of the actuator overhanging tip is also shown, indicating holes created in it to reduce forces exerted on the actuator by the jet flow.

Based on this observation, we proceeded to design and fabricate modified actuator structures that could provide a higher stiffness in the plane perpendicular to the jet flow. This was accomplished in several ways. First, we modified the design of the actuator so that support anchors for the moving mass were spread out over the entire area of the actuator, thus effectively increasing the torsional spring constant. An improvement of an order of magnitude could be achieved in this new design. Second, we also reduced the distance from the anchors to the two ends of the actuator from about 400 μm to about 200 μm . This also increased the stiffness of the actuator and effectively made it more resistant to tilting. In some samples we also increased the thickness of the actuator from about 12 μm to about 14 μm . Finally, in order to reduce the amount of force acting on the actuator tip, we created holes in it so that there is a path for the oncoming flow to pass through the actuator. Figure 14 shows a SEM view of one of the second-generation actuators, and a close-up view of the tip of the actuator overhanging the glass substrate showing the holes created in it. The device is 1.3mm wide, 10 μm thick, and has a head that overhangs the glass substrate by ~200 μm to allow it to enter the jet flow. We have also made devices that are thicker than the 10 μm device shown here.

Table 2: Dimensions of the first- and second-generation designs of the electrostatic microactuator.

		Old design	New design
Beam	width	3 μm	6 μm
	thickness	12 μm	
	length	200 μm	300 μm
Anchor distance		135 μm	750 μm
Tip/tail to anchor distance		490/380 μm	250/65 μm

Table 2 summarizes the dimensions for the old and new designs. We have performed FEM simulations on these two generation designs. These simulations have shown that the new design is at least 20 times stiffer than the old design when a force is applied to the tip of the actuator head as shown in Figure 6. We believe that the real improvement is even more significant than this because the reduced area of the overhanging plate (due to holes etched in the actuator tip) in the new design results in a smaller F_z . The microactuator is driven into resonance electrostatically by large comb drives. Each microactuator can be controlled individually, and can be resonated to an amplitude of larger than 60 μm peak to peak at a resonant frequency of 5kHz using a 20V AC signal and a 20V DC bias. Table 3 summarizes the measurement results under different bias voltages for the second-generation actuators. Note that the microactuator tip is "meshed" with a large number of holes in order to reduce the vertical forces induced on it by the high speed flow. This will also reduce the possibility of clamping the actuator during operation.

Table 3: Measured results for the second-generation microactuator.

Bias (ac + dc)	Resonant Frequency (kHz)	Amplitude ($\mu\text{m p-p}$)
7.5+7.5	5.18	12
10 + 10	5.16	22
12.5+12.5	5.16	28
15+15	5.16	36
17.5+17.5	5.16	52
20+20	5.16	70

Recent testing of the new actuator with the HSJF at IIT has demonstrated significant improvements over the earlier design. The device was tested in flow speeds corresponding to those occurring during screech ($\sim 400\text{m/s}$). At these conditions, most of the devices resonated successfully for 20 to 40 seconds before getting clamped. These devices were located very close to the jet lip ($< 100\mu\text{m}$). Furthermore, no structural damage was observed for these devices. Figures 15 (a) and (b) show the measured power spectra of the disturbance for the jet velocity of 28m/s and 45m/s , respectively. All streamwise disturbance measurements are obtained using a hot-wire anemometer placed at $x/d = 0.3$ (where x is the distance between the hot-wire and the jet lip and d is the jet diameter). These spectra were obtained when exciting the shear layer using a single MEMS device at various radial locations with respect to the jet lip (r_{off}). As can be seen from Figure 15(a), at low-speed jet velocity (28m/s), a strong peak in the spectrum is observed for all values of r_{off} , that is the actuator location was from $-320\mu\text{m}$ to $80\mu\text{m}$. It is interesting to note that only $r_{\text{off}} = 0$ and $80\mu\text{m}$ does the actuator actually penetrate the shear layer. Thus the second-generation actuators are capable of exciting the shear layer at low speeds without direct protrusion. At higher jet velocity (45m/s), Figure (b) also shows a strong peak at the resonant frequency of the actuator ($\sim 5\text{kHz}$). However, the peaks are only observed for the radial actuator positions where it penetrates the shear layer. It is important to compare the results of Figure 15(b) to the fact that the actuators based on the first-generation design were unable to introduce disturbances into the shear layer at jet speeds higher than 36m/s . To further investigate the influence on the effectiveness of the MEMS device as the jet speed increases, spectra were also obtained at the jet speed of 100m/s when $r_{\text{off}} = 80\mu\text{m}$. Those results are included with the results for velocities of 28m/s and 45m/s in Figure 16. It shows the MEMS devices are able to excite a flow disturbance at the velocity of 100m/s . However, this peak is considerably smaller in magnitude than that peak observed at jet speed of 45m/s and 28m/s . From a fluid mechanical point of view, the success of the MEMS actuators in introducing the desired disturbance into the shear layer depends on the receptivity of the shear layer to this type of mechanical excitation. In particular, the effect of a large number of geometrical and physical parameters on receptivity to the MEMS actuators need to be understood in order to achieve effective design of the actuators which would work at screech conditions. Through the previous experiment, we could expect to gain better understanding about the receptivity of the shear layer to MEMS actuators. Further experiments will be conducted at IIT in the future.

VII. Conclusions

During the past two years, we accomplished several objectives of the original project, while several others are still under study and are being researched. As mentioned before, one of the main goals of this research was to design, fabricate, and test a miniature actuator array using silicon micromachining techniques for use in fluid mechanics research in general, and for the control of screech in high speed jets in particular. The project has been successful in terms of this objective. A microactuator-microsensor system has been fabricated. This system contains an array of small microactuators and hot-wire anemometers fabricated using p++ bulk-silicon dissolved wafer process. The devices have operated as designed and actuation amplitudes of at least $60\mu\text{m}$ peak to peak at frequencies around 5kHz have been achieved. In addition, a custom-designed circuit board has been developed for monitoring the operation of the micro-mechanical system *in-situ* during actual use on a high-speed jet flow (HSJF) system. The microactuator went through several design cycles to circumvent problems observed when it was actually operated in the harsh environment of the high-speed jet. The supersonic jet creates a very turbulent environment around the actuator, especially when the actuator is pushed into the mean flow of the jet. This extreme turbulence condition, together with the fact that the flow contains many particulates, caused the original actuator to stop working. The redesigned actuators have now been extensively tested at IIT, and are much more robust than their predecessors. Another challenge that had to be overcome and took some effort, was that of developing the electronics that could be incorporated into each actuator board to detect the very small motion of each actuator while in operation. The AC current generated when the actuator was operating was in the picoampere range. The detection electronics had to be small enough, yet sensitive enough, to measure this small change in current. This detection electronics was also successfully designed and tested in the HSJF. Furthermore, a packaging system, including the printed-circuit board and an attachment technique, had to be developed that was compatible with the small size of the actuator and the jet facility. This was also successfully accomplished. Our colleagues at IIT have also developed an optical detection set up to visually observe the actuator motion while the jet is on. All of these developments have made it possible to routinely test and observe the operation of these actuators on the high-speed jet. Several of the most recent tests have successfully demonstrated that a disturbance can be created at the desired frequency and coupled into the jet at velocities approaching 100m/s even when the actuator is pushed into the mean jet flow. This is a very significant result and represents the first microactuator that has operated under such harsh conditions. In spite of all of these accomplishments, we have not yet been able to successfully control and stop screech in high speed jets. This is a very complicated and difficult task which we are still pursuing. Many more measurements and experiments have to be conducted to really understand the interaction between these actuators and the jet. These experiments are now underway and will continue into the future. All the necessary components for conducting such experiments are now in place. The goal of controlling screech using a closed-loop feedback system remains to be achieved.

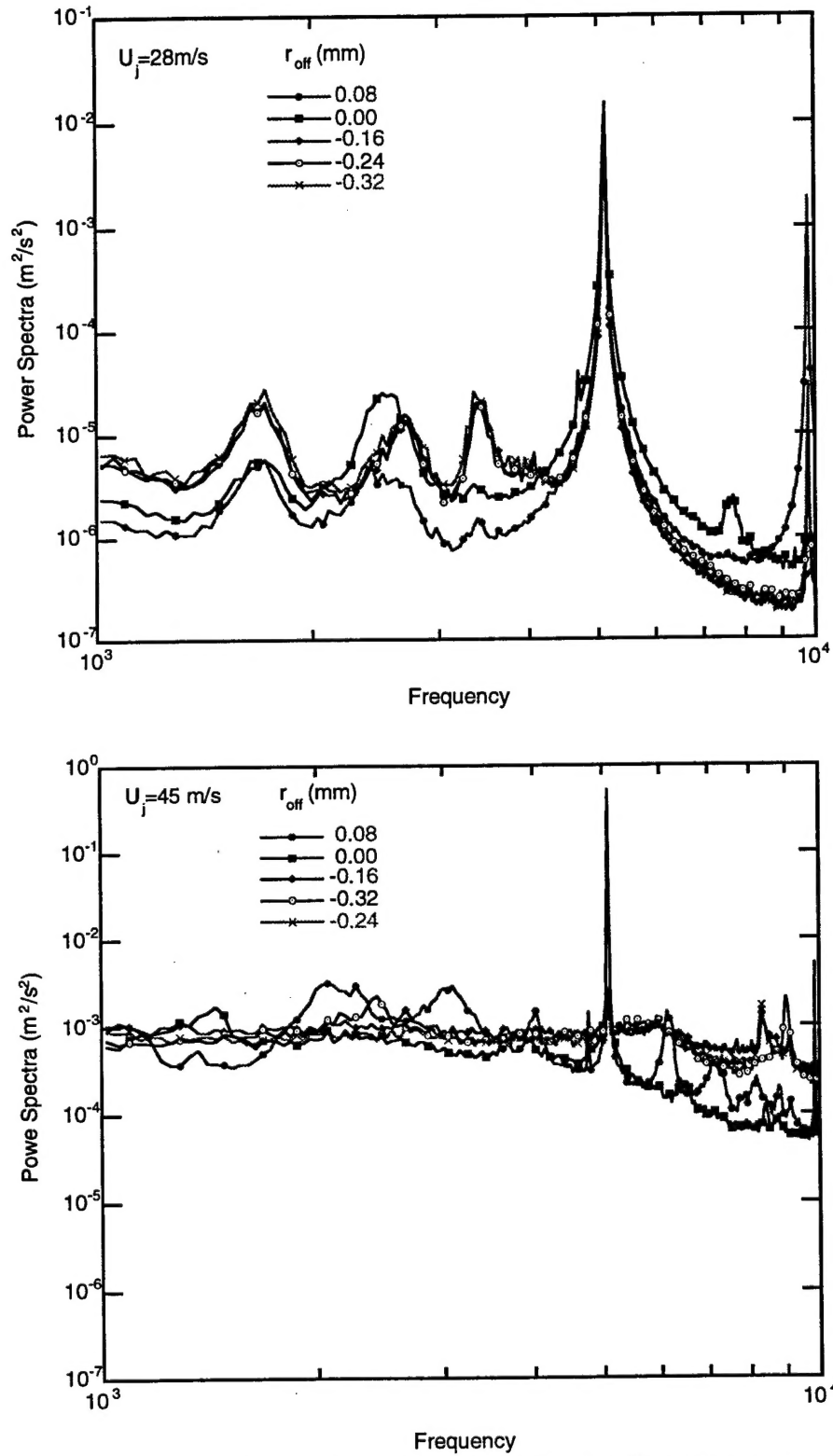


Figure 15: Effect of actuator location on the streamwise velocity disturbance spectrum at $x/d=0.3$ and $U/U_j=0.5$: (a) $U_j=28 \text{ m/s}$ and (b) $U_j=45 \text{ m/s}$.

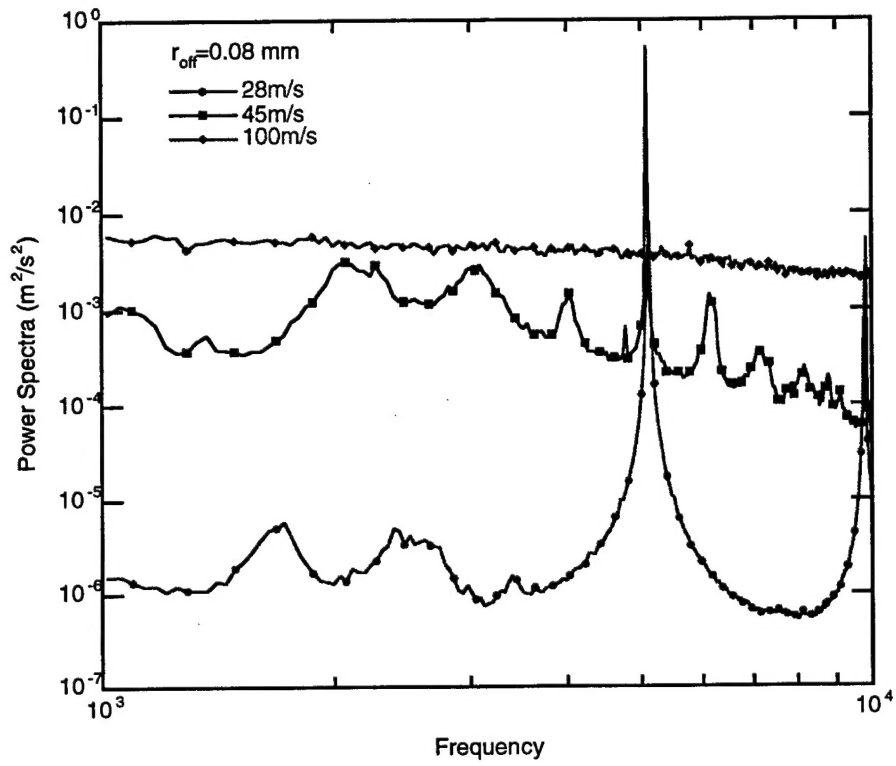


Figure 16: Effect of jet speed on the disturbance spectrum for a fixed actuator location (r_{off}) of $80\mu\text{m}$.

VIII. References

- [1] D.W. Bechert, and B. Stahl, "Shear Layer Excitation, Equipment vs. Theory," DFVLR TR No. DFVLR-FB pp. 84-26, 1984
- [2] D.G. Crighton, "The Kutta Condition in Unsteady Flow," *Ann. Rev. Fluid Mech.*, 17, pp. 411-445, 1985
- [3] R.E. Drubka, P. Reisenthel, and H.M. Nagib, "The Dynamics of Low Initial Disturbance Turbulent Jets," *Phys. Fluids A*, 1, pp. 1723-1735, 1989
- [4] Y.B. Gianchandani, and K. Najafi, "A Bulk Silicon Dissolved Wafer Process for Microelectromechanical Systems," *IEEE/ASME J. Micro Electro Mechanical Systems*, Vol. 1, No. 2, pp. 77-85, June 1992

IX. Personnel Supported

- 1. Professor Khalil Najafi: Principal Investigator. Supported at a level of 10% through cost sharing provided by the University of Michigan
- 2. C.C. Huang, Graduate Student Research Assistant, 50% Appointment: Microactuator design, simulation, and fabrication

X. Publications

C. Huang, J. Papp, K. Najafi, and H. M. Nagib, "A Microactuator System For The Study And Control Of Screech In High Speed Jets," *Proceedings, IEEE-MEMS-96 Workshop*, pp. 19-24, San Diego, CA, Feb. 1996

XI. Interactions/Transitions

None

XII. New Discoveries, Inventions, or Patent Disclosures

None